Enhanced Analysis of Multiconductor Nanostructured Devices via a Compact Block FDTD/VFETD Method

Nikolaos V. Kantartzis[1], Theodoros T. Zygiridis[2], and Theodoros D. Tsiboukis[1]
[1]Dept. of Electrical & Computer Engineering, Aristotle University of Thessaloniki, 54124 Thessaloniki, Greece
[2]Dept. of Informatics & Telecommunications Engineering, University of Western Macedonia, 50100 Kozani, Greece
E-mail: kant@auth.gr; tzygiridis@uowm.gr; tsibukis@auth.gr

***Abstract*—A reduced-order modeling FDTD/VFETD technique is presented in this paper, for the accurate and cost-effective study of multiconductor nanoscale structures. The novel algorithm blends a compact stencil-optimized discretization process with general vector finite elements and partitions the domain into tightly-coupled blocks. A key asset is that both approaches are time-advanced independently while their state-space models are derived via a Krylov-based scheme with scaled Laguerre functions, which drastically decreases the order of the transfer matrix. Numerical results from various nanocomposite devices validate the hybrid method and reveal its applicability.**

***Index Terms*—Carbon nanotubes (CNT), FDTD methods, FETD schemes, model-order reduction, nanostructured devices.**

I. Introduction

The accurate evaluation of the electromagnetic response of nanostructured components and carbon nanotube (CNT) systems is strongly associated to the consistent representation of their size by the pertinent sampling rates [1], [2]. In particular, when multiconductor setups are involved, it is critical to quantify any intermodulation issues, as ever-increasing switching speeds drive signal bandwidths to tens of gigahertz at all levels of high-density packaging. Considering that many of these devices must be continually reconfigured, it is apparent that computational models can significantly restrict unduly construction expenses. However, their application is not always undemanding, because of the convoluted features and the nonlinear character of the preceding systems. To this objective, an assortment of robust schemes has been hitherto developed to mitigate the analysis' total complexity [3]-[6].

In this paper, a hybrid 3-D algorithm for the comprehensive macromodeling of multiconductor nanocomposite applications is introduced. The new method combines a compact-stencil finite-difference time-domain (FDTD) technique with a modified vector finite-element time-domain (VFETD) formulation, which are updated independently and separate the domain into flexible local blocks coupled by the proper continuity conditions. The decrease of the discrete model is achieved via a Laguerre-oriented Krylov-subspace model-order reduction scheme that splits all subspace vectors into their electric field intensity and magnetic flux density parts at a stage prior to any simulation. Thus, the number of unknown variables is seriously confined and high levels of accuracy as well as resources economy are attained, even when sub-wavelength details are to be considered. These advantages are successfully certified by diverse nanostructured setups with complex geometries, large electrical sizes, and arbitrarily-curved interfaces.

II. Reduced-Order-Model FDTD/VFETD Technique

Starting from the first part of the 3-D hybrid method, the principal aim is to construct an efficient FDTD discretization, based on a generalized curvilinear dual-lattice regime. Hence, a family of compact spatial and temporal approximators is introduced as

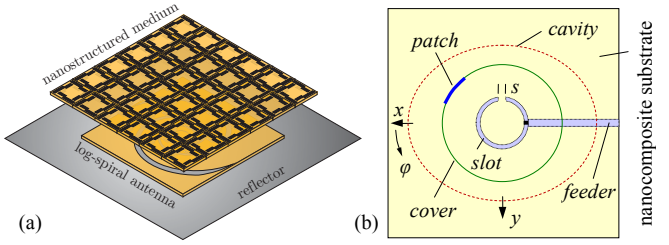

Fig. 1. (a) A log-spiral antenna with a multiconductor nanostructured superstrate and (b) a hemi-ellipsoidal cavity-backed antenna with a nanocomposite substrate.

$$\mathbf{L}_{\xi}^{K}\left[f\big|_{p}^{n}\right]=\sum_{r=1}^{K}\frac{(\Delta\xi)^{4r+3}}{3^{2r-1}(5r+2)!}\left(f\big|_{p+r-1/2}^{n}-f\big|_{p-r+1/2}^{n}\right), \quad (1)$$

$$\mathbf{T}^{M}\left[f\big|_{p}^{n}\right]=\Xi^{-1}(\Delta t)\left(f\big|_{p}^{n+1/2}-f\big|_{p}^{n-1/2}\right)+\sum_{s=2}^{M}\frac{\partial^{s}f}{\partial t^{s}}\bigg|_{p}^{n} \quad (2)$$

where $\xi\in(u, v, w)$ coordinate system, $p\in(i, j, k)$, $\Delta\xi$ is the spatial increment, Δt the time-step, r indicates specific grid points, and

$$\Xi(\Delta t)=(2q+5)(\Delta t)^{M-1}-3(q+4)(\Delta t)^{M} \quad \text{for } q\in[0,1/2], \quad (3)$$

a weighting function for broadband adjustments. Compact forms (1) and (2), of order K and M, are then applied to Maxwell's equations in the usual way to create an enhanced FDTD model. In fact, their tensorial profile leads to a locally-refined dual grid with a finite number of uniquely located nodal patterns, which can precisely describe multiconductor nanoscale devices, as in Fig. 1.

Concerning the modified VFETD algorithm, we define

$$\mathbf{G}_1=\sum\nolimits_i \mathcal{G}_1^i\mathbf{w}_i^{(1)} \quad \text{and} \quad \mathbf{G}_2=\sum\nolimits_j \mathcal{G}_2^j\mathbf{w}_j^{(2)}, \quad (4)$$

with $\mathbf{G}_1=[\mathbf{E}, \mathbf{H}]$, $\mathbf{G}_2=[\mathbf{D}, \mathbf{B}, \mathbf{J}_c]$ the electric/magnetic intensities, fluxes, and external source vectors, and $\mathbf{w}^{(1)}$, $\mathbf{w}^{(2)}$ the basis functions [7]. Also, $\mathcal{G}_1=[\mathcal{E}, \mathcal{H}]$ denotes the circulation of $\mathbf{G}_1$ along edge$\{i\}$ and $\mathcal{G}_2=[\mathcal{D}, \mathcal{B}, \mathcal{J}_c]$ the $\mathbf{G}_2$ flux through facet$\{j\}$. Plugging (4) in Ampere's and Faraday's law, one gets

$$\sum\nolimits_i \mathcal{H}^i\nabla\times\mathbf{w}_i^{(1)}=\sum\nolimits_j\left(\partial_t\mathcal{D}^j+\mathcal{J}_c^j\right)\mathbf{w}_j^{(2)}, \quad (5a)$$

$$\sum\nolimits_i \mathcal{E}^i\nabla\times\mathbf{w}_i^{(1)}=-\sum\nolimits_j \partial_t\mathcal{B}^j\mathbf{w}_j^{(2)}. \quad (5b)$$

To simplify the above formulas, one may employ the properties of differential forms. So, in matrix notation, (5a) and (5b) become

$$\partial_t\boldsymbol{\mathcal{D}}=\mathbf{Y}\boldsymbol{\mathcal{H}}-\boldsymbol{\mathcal{J}}_c \quad \text{and} \quad \partial_t\boldsymbol{\mathcal{B}}=-\mathbf{Y}\boldsymbol{\mathcal{E}}, \quad (6)$$

for $\mathbf{Y}$ the circulation matrix occupied either by unity or zero elements. The system of (6) is completed by the correct association of fluxes with fields and the following constitutive relations

$$\sum\nolimits_j \mathcal{D}^j\mathbf{w}_j^{(2)}=\varepsilon\sum\nolimits_i \mathcal{E}^i\mathbf{w}_i^{(1)}, \quad (7a)$$

$$\sum\nolimits_j \mathcal{B}^j\mathbf{w}_j^{(2)}=\mu\sum\nolimits_i \mathcal{H}^i\mathbf{w}_i^{(1)}. \quad (7b)$$

Time advancing in (6) is conducted via a leapfrog-like scheme and is completely independent of the time-update procedure in the compact FDTD approach, on condition that the minimum Courant limit is considered for the selection of both temporal increments.

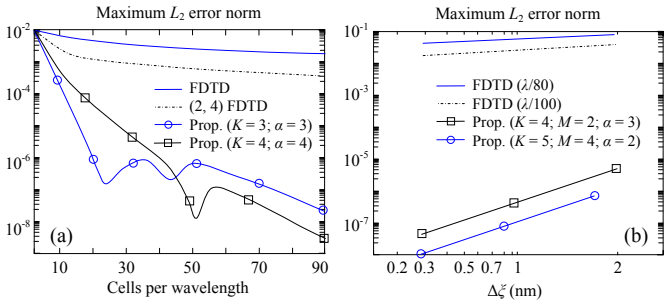

Fig. 2. Maximum L_2 norm versus (a) mesh resolution and (b) spatial increment.

Next, the domain is divided into simple FDTD or VETD blocks, related to the problem details, and coupled by the suitable continuity conditions. This topology allows the accurate treatment of periodic nanoscale components, CNT patterns, and multiconductor arrangements with very limited memory requirements.

Having specified the hybrid methodology and gathering all unknown variables in vector $\mathbf{x}(t)$, one gets the linear system of

$$\mathbf{Z}\frac{d\mathbf{x}}{dt} = -\mathbf{F}\mathbf{x} + \mathbf{Q}\mathbf{b} \qquad \text{and} \qquad \mathbf{s} = \mathbf{P}^T\mathbf{x}\,, \tag{8}$$

where $\mathbf{F}$ is a $N\times N$ sparse matrix with discretization data, $\mathbf{Z}$ is a $N\times N$ matrix with media information, and $\mathbf{Q}$, $\mathbf{P}$ matrices containing the coupling coefficients for the domain's neighboring blocks. To lessen the size of $\mathbf{x}$ in (8), without actually affecting the overall accuracy, a model-order reduction approach is developed. The principal concept is to construct another linear system with the same transfer function between $\mathbf{b}$ and $\mathbf{s}$, but with a different vector $\mathbf{x}$. In particular, the state-space model (8), with Λ inputs yields the $\Lambda\times\Lambda$ impulse response transfer matrix $\mathbf{h}(t)$, that is expanded as

$$\mathbf{h}(t) = \sum_{l=0}^{\infty}\mathbf{A}_l\vartheta_l^m(t)\,, \tag{9}$$

by the $\vartheta_l(t) = (2m)^{1/2}e^{-mt}\mathcal{L}_l(2mt)$ scaled Laguerre functions (for l = 0,1,2,…), with $m > 0$ a scaling parameter and $\mathcal{L}_l(t)$ the Laguerre polynomial of order l. After some algebra, we acquire matrices

$$\mathbf{V} = -(m\mathbf{Z}+\mathbf{F})^{-1}(m\mathbf{Z}-\mathbf{F}) \qquad \text{and} \qquad \mathbf{R} = (m\mathbf{Z}+\mathbf{F})^{-1}\mathbf{Q}\,, \tag{10}$$

which are used for the extraction of the $N\times\alpha\Lambda$ Krylov subspace $\mathbf{K} = [\mathbf{R},\mathbf{V}\mathbf{R},\mathbf{V}^2\mathbf{R},\ldots,\mathbf{V}^{\alpha-1}\mathbf{R}]$, with factor α denoting the order of reduction. Also, during the derivation of $\mathbf{K}$, matrices (10) generate the $N\times\alpha\Lambda$ column-orthogonal matrix $\mathbf{U}$ through the block Arnoldi process [6]. This formulation provides the reduced-order system of

$$\tilde{\mathbf{Z}}\frac{d\mathbf{y}}{dt} = -\tilde{\mathbf{F}}\mathbf{y} + \tilde{\mathbf{Q}}\mathbf{b} \qquad \text{and} \qquad \mathbf{s} = \tilde{\mathbf{P}}^T\mathbf{y}\,, \tag{11}$$

where $\mathbf{y}(t)$ is the reduced $a\Lambda$ vector of unknown variables, and

$$\tilde{\mathbf{Z}} = \mathbf{U}^T\mathbf{Z}\mathbf{U}\,, \quad \tilde{\mathbf{F}} = \mathbf{U}^T\mathbf{F}\mathbf{U}\,, \quad \tilde{\mathbf{Q}} = \mathbf{U}^T\mathbf{Q}\,, \quad \tilde{\mathbf{P}} = \mathbf{U}^T\mathbf{P}\,. \tag{12}$$

So by properly selecting α, m and applying (1)-(7), the proposed wideband technique significantly minimizes dispersion errors (Fig. 2), and attains a notable decrease of the computational overhead.

III. Numerical Results – Conclusions

The novel method is validated by several multiconductor nanoscale devices. The first problem deals with the performance enhancement of a miniaturized 10×10 mm log-spiral antenna via an Appl. Science™ CNF superstrate, as in Fig. 1(a). For the discretization, we select m = 5 to obtain a 86×86×28 FDTD grid (K = 3, M = 2) for the superstrate and a 490,362 VFETD mesh for the radiator and the rest of the domain. Figure 3(a) gives the H_y variation and Fig. 3(b) the intermodulation voltage between the two spirals for diverse α. As detected, the hybrid algorithm overwhelms the usual FDTD method, even for a 85% denser lattice

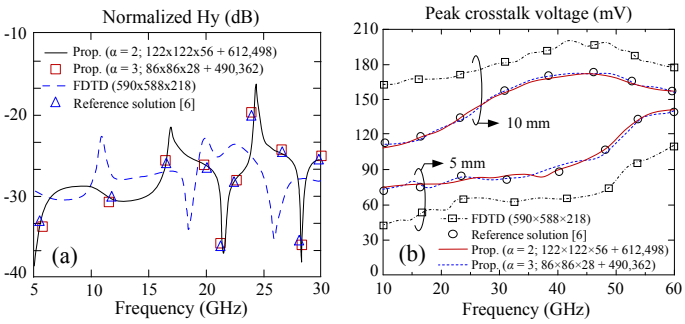

Fig. 3. (a) Variation of the normalized H_y component and (b) intermodulation voltage for two different distances of the nanostructured superstrate in Fig. 1(a).

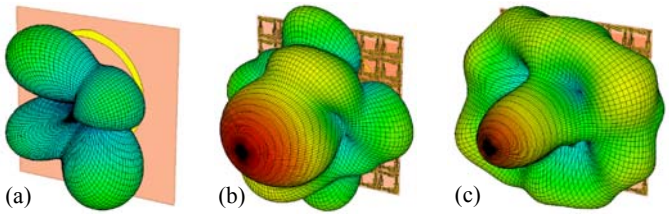

Fig. 4. Directivity enhancement of the log-spiral nanoantenna via a nanoscale superstarte. (a) initial, (b) superstrate distance 5 mm, (c) superstrate distance 10 mm.

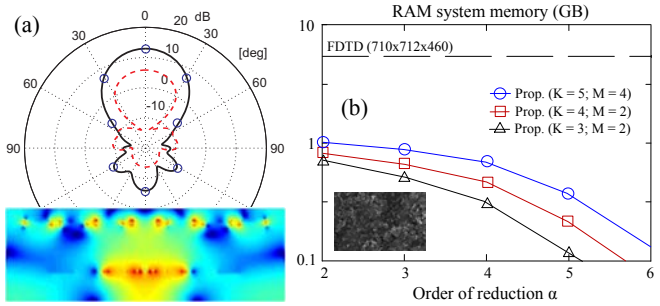

Fig. 5. (a) Radiation pattern (straight line: proposed; circles: [2]; dashed line: FDTD) and E_z snapshot and (b) system memory versus order-reduction factor α.

and an 80% higher arithmetic complexity. Also, Fig. 4 shows the serious directivity improvement. The second structure is the hemiellipsoidal antenna of Fig. 1(b) with a multiconductor Nanotech™ CNT substrate. For α = 4, m = 6, the grid comprises 78×65×20 FDTD cells and 4.982×10^5 degrees of freedom. Results for the radiation pattern and an E_z magnitude snapshot are presented in Fig. 5(a), while Fig. 5(b) shows the significant decrease of the system memory needs (likewise for CPU time) in terms of α factor.

References

[1] A. Breda, D. Esseni, A. Paussa, R. Specogna, F. Trevisan, and R. Vermiglio, "Comparison between pseudospectral and discrete geometric methods in nanoscale devices," *IEEE Trans. Magn.*, vol. 48, no. 2, pp. 203–206, 2012.

[2] P. Lamberti, M. Sarto, V. Tucci, and A. Tamburrano, "Robust design of high-speed interconnects based on an MWCNT," *IEEE Trans. Nanotechnol.*, vol. 11, no. 4, pp. 799–807, Nov. 2012.

[3] T. Wittig, I. Munteanu, R. Schuhmann, and T. Weiland, "Two-step Lanczos algorithm for model order reduction," *IEEE Trans. Magn.*, vol. 38, no. 2, pp. 673–676, 2002.

[4] C. Scheiber, A. Schultschik, O. Bíró, R. Dyczij-Edlinger, "A model order reduction method for efficient band structure calculations of photonic crystals," *IEEE Trans. Magn.*, vol. 47, no. 5, pp. 1534–1537, 2011.

[5] A. Vion, R. Sabariego, and C. Geuzaine, "A model reduction algorithm for solving multiple scattering problems using iterative methods," *IEEE Trans. Magn.*, vol. 47, no. 5, pp. 1470–1473, 2011.

[6] P. Sumant, H. Wu, A. Cangellaris, and N. Aluru, "Reduced-order models of FE approximations of electromagnetic devices exhibiting statistical variability," *IEEE Trans. Antennas Propag.*, vol. 60, no. 1, pp. 301–309, 2012.

[7] A. Bossavit, "Generating Whitney forms of polynomial degree one and higher," *IEEE Trans. Magn.*, vol. 38, no. 2, pp. 341–344, 2002.